The Computation of the Effects of Harmonic Currents on Transformers using a Coupled Electromagnetic-Thermal FEM Approach

Johan Driesen, Ronnie Belmans, Kay Hameyer
Katholieke Universiteit Leuven, Dep. EE (ESAT), Div. ELEN
Kardinaal Mercierlaan 94, B-3001 Leuven, Belgium
Phone: +32/16/32.10.20 Fax: +32/16/32.19.85
e-mail: johan.driesen@esat.kuleuven.ac.be

Abstract: The use of coupled electromagnetic-thermal finite element methods to estimate the thermal impact of power system harmonics on transformers is illustrated. At first, the magnetic modelling of transformers is outlined with attention for the core, windings and the external source or loads. Particular attention is paid to the foil windings. The loss computation and the thermal modelling is discussed. The calculation of the global coupled problem using a mixed frequency and time domain approach, for the steady-state as well as for a long-term transient evolution, is treated. These methods are applied to a 30 kVA distribution transformer. The results are compared with measurements. A derating procedure based on the simulated hot spot temperature is presented.

Keywords: transformers, power quality problems, power system harmonics, K-factors, finite element methods, coupled problems.

I. INTRODUCTION

Transformers carrying power system harmonics exhibit additional load losses, yielding higher hot spot temperatures. Reducing the maximum apparent power transferred by the transformer, often called derating, is required when such power quality related problems occur [1-5]. To estimate the impact of a harmonic load already in the design stage, a finite element method (FEM) field calculation can be employed. The FEM models can be applied in a derating produre or to estimate the time evolution of the thermal overload under certain conditions.

The behaviour of an electromagnetic device, and in particular a transformer, are best modelled using coupled electromagnetic-thermal numerical field models. On one side, the electromagnetically based losses are the source terms for the thermal problem. On the other side, the specific electromagnetic material parameters are temperature dependent. It can be noted that there are large differences in time constants of the magnetic and thermal field. This yields a 'stiff' transient problem, requiring a special solution approach.

II. MAGNETIC FIELD MODELLING

A. FEM frequency domain computation

1) Single frequency magnetic fields: The magnetic fields are simulated using the magnetic vector potential $\boldsymbol{A}$ [6]:

$$\boldsymbol{B}(t) = \nabla \times \boldsymbol{A}(t) \tag{1}$$

After substituting (1) in the Maxwell equations, the following equation for a 2D time dependent magnetic field is obtained:

$$\nabla \cdot \left(\upsilon(A)\nabla A\right) - \sigma(T)\frac{\partial A}{\partial t} = -J_s = -\sigma(T)V_s \tag{2}$$

with
- A the z-component of the vector potential
- T temperature
- υ magnetic reluctivity (non-linear due to ferromagnetic saturation)
- σ electrical conductivity (thermally dependent)
- J_s source current density
- V_s source voltage

The temperature dependence of several parameters in the magnetic field equation may cause significant changes in their solution, for instance in the skin effects and loss distributions. Therefore, this equation is inherently coupled to the thermal field distribution.

To compute quasi-periodic *AC* magnetic fields, it is interesting to substitute the vector potential A in (2) by:

$$A(t) = \underline{A}(t)e^{j2\pi f t} = \underline{A}(t)e^{j\omega t} \tag{3}$$

Here, the magnetic vector potential is split into a time dependent phasor and an oscillating harmonic function. The frequency of the oscillation f is the fundamental mains frequency. Then, the phasor describes the long-term magnetic field evolution related to slow time constants, e.g. due to thermally coupled effects. A similar substitution is obtained for the source quantities. Eq. (2) becomes a complex equation:

$$\nabla \cdot \left(\upsilon(\underline{A})\nabla \underline{A}\right) - j\omega\sigma\left(\underline{A} + \frac{\partial \underline{A}}{\partial t}\right) = -\underline{J}_s = -\sigma \underline{V}_s \qquad (4)$$

The remaining dynamic phenomena in this equation take place on the slow (thermal) time scale; the fast oscillations have been eliminated. The reason for this substitution is to avoid numerical problems due to stiffness when the small magnetic and large thermal time constants are to be combined in a coupled simulation. For the steady-state field, the time derivative of the phasor is omitted.

2) Multi-harmonic magnetic fields: When the currents and/or voltages involved are not sinusoidal, but still quasi-periodic, the magnetic field will contain harmonic components as well. In that case, it is better to substitute the time-dependent magnetic vector potential by a sum of harmonic components:

$$A(t) = \sum_{h=1}^{N} \underline{A}_h(t) e^{jh\omega t} \qquad (5)$$

Substituting (5) in (2) yields a set of equations of the form (4), as the frequency components are orthogonal. These equations are then theoretically coupled through the ferromagnetic non-linear reluctivity [7].

3) Magnetic saturation: In real power systems, the internal impedance of the supply system is low enough to keep the voltage distortion relatively limited, even when high current distortion is found. Since the magnitude of the magnetic flux is inversely proportional to the frequency, the fundamental component dominates the transformer's magnetic field evolution. As a consequence, it is reasonable to assume that the saturation of the ferromagnetic core is determined by the fundamental field component. The set of equations obtained by substituting (5) in (2) can then be split into [7]:

$$\nabla \cdot \left(\upsilon(\underline{A}_1)\nabla \underline{A}_1\right) - j\omega\sigma\left(\underline{A}_1 + \frac{\partial \underline{A}_1}{\partial t}\right) = -\underline{J}_{s,1} = -\sigma \underline{V}_{s,1} \quad (6)$$

$$\nabla \cdot \left(\upsilon(\underline{A}_1)\nabla \underline{A}_h\right) - jh\omega\sigma\left(\underline{A}_h + \frac{\partial \underline{A}_h}{\partial t}\right) = -\underline{J}_{s,h} = -\sigma \underline{V}_{s,h} \quad (7)$$

with $h>1$

Eq. (6) is non-linear and has to be solved first to fix the saturation level for the remaining linear equations (7), which can be solved in parallel.

In the derivation of these frequency domain magnetic field equations, it is assumed that the saturation level remains constant, which is an approximation. Alternatively, a far more complicated harmonic balance algorithm can be used [7].

The finite element discretisation methodology is applied on the equations (4) and (6-7). The time derivative is generally approximated by a first order difference. Eventually, the algebraic system to be solved in every time step is obtained.

B. Transformer model

In general, the magnetic field model of the transformer can be distinguished into three parts: the core, the windings and the surrounding 'air'.

1) Air: In principle, the surrounding air is entirely to be included in the model as it contains the leakage flux. In practice, a Kelvin transformation is applied to the domain at a certain distance, yielding an 'open boundary' [8].

2) Core: The ferromagnetic iron core can be modelled using an anisotropic reluctivity. It is possible to include the effect of iron losses by using a complex reluctivity with a phase angle due to the delay between the *B* and *H* vector [9].

3) Winding: The representation of the winding is related to the modelling of skin effect. Therefore, a stranded winding is represented using a uniform scaled current density. The induction term in the magnetic field equation, representing the eddy currents, is neglected. This approximation is not correct for massive windings, such as foils. They exhibit eddy currents and a non-uniform current density distribution even for the fundamental frequency. The skin effect imposes the necessity to mesh the foil winding cross-sections individually using elements having a size which is smaller than this skin depth. Especially in the models with higher current harmonics, this may yield large finite element.

C. External circuit model

The current source densities at the right-hand side of the magnetic field equations are associated to another set of equations, the circuit equations [6]. For a transformer, typically two parts have to be represented in this way: the supply side and the load. The supply is modelled by a voltage source with the fundamental frequency and an internal impedance. At harmonic frequencies, the voltage source is replaced by a short circuit (Fig. 1). The load, e.g. a bridge rectifier, is modelled by a set of current sources, one for each harmonic frequency (Fig. 2). The magnitude and the phase of each current source are determined by the complex spectrum of the load current.

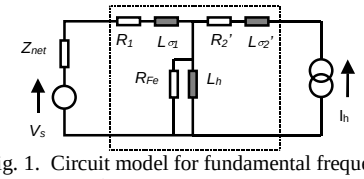

Fig. 1. Circuit model for fundamental frequency (the part in the frame is included in the FEM model).

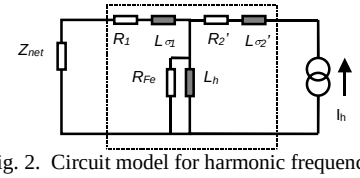

Fig. 2. Circuit model for harmonic frequencies.

III. THERMAL FIELD MODELLING

A. Thermal field computation

The transient thermal field is calculated by means of a Poisson-like differential equation:

$$\nabla \cdot (\lambda \nabla T) - \rho c \frac{\partial T}{\partial t} = -q(A,T) \tag{8}$$

with T temperature
λ thermal conductivity
ρ mass density
c heat capacitance
q heat source density (often a non-linear and coupled expression)

It is to be extended with mixed boundary conditions, representing convective cooling:

$$-\lambda \frac{\partial T}{\partial n} = h_c (T - T_\infty) \tag{9}$$

The determination of the heat transfer coefficients h_c towards the medium with temperature T_∞ can become troublesome as it requires the knowledge of the cooling fluid flow regime. Based on the estimation of this state, modelled by a Reynolds number associated with the relevant geometrical configuration, a Nusselt number is calculated, which is a dimensionless heat transfer coefficient [10]. Thus, the air must not be meshed in the thermal problem.

The equations (8) and (9) are discretised in space and time by means of the FEM.

B. Transformer model

It depends on the cooling system, which construction parts have to be considered in the thermal model. For instance, for air-cooled transformers, the core and the windings can be treated almost separately. The core can be represented as an anisotropic solid part due to the laminations.

The windings, being a complicated composite of insulation and conductors, are usually represented by means of equivalent (anisotropic) conductive materials. Several options exist:

- Isotropic composite: Some types of conductors, such as dense stranded windings can be represented by a single isotropic thermal conductivity, calculated using a weighted average, based on volume fractions:

$$\lambda_{eq} = \frac{\lambda_{cond} V_{cond} + \lambda_{insul} V_{insul}}{V_{cond} + V_{insul}} \tag{10}$$

  Similar formulae are to be used for ρ and c.
- Anisotropic composite: Other types of conductors, such as dense foil windings are better represented by an anisotropic thermal conductivity. Two main directions are distinguished for this type of coil, namely in the foil plane (axial λ_a/tangential λ_t) and perpendicular to it (radial λ_r). In the foil plane directions, the conductor and insulation layers with thickness d are in parallel. The conductor value dominates:

$$\begin{aligned} \lambda_a = \lambda_t &= \frac{\lambda_{cond} d_{cond} + \lambda_{insul} d_{insul}}{d_{cond} + d_{insul}} \\ &\approx \lambda_{cond} \frac{d_{cond}}{d_{cond} + d_{insul}} \end{aligned} \tag{11}$$

  In the perpendicular direction, the conductor and insulation layers with thickness d are in series. The insulator value dominates:

$$\begin{aligned} \lambda_r &= \frac{1}{\left(\frac{1}{\lambda_{cond} d_{cond}} + \frac{1}{\lambda_{insul} d_{insul}} \right) (d_{cond} + d_{insul})} \\ &\approx \lambda_i \frac{d_{insul}}{d_{cond} + d_{insul}} \end{aligned} \tag{12}$$

- Alternatively, a special type of element relations can be used, in which the thin insulation layers are modelled as a thermal contact resistance layer [11]. This approach increases the number of degrees of freedom.

IV. LOSS COMPUTATION

The transformer losses are distinguished into the no-load losses and the load losses. The no-load losses are almost entirely core iron losses. These are calculated by the FEM by the summation of the uniform loss densities within the elements. The loss density distribution is obtained by estimating the iron loss values as a function of the magnetic flux density.

The load losses, which are mostly Joule losses, can be split into three types [3]:

- *DC* losses
- Additional *AC* losses
- Additional stray losses (in structural parts)

Current harmonics cause an increase of the additional *AC* losses and the stray losses. For a stranded winding, with a non-prominent skin effect, the additional *AC* losses rise proportionally to the square of the harmonic order, which led to the traditional definition of the *K*-factor [4]. The stray losses are very much construction dependent.

The Joule losses in the windings are calculated by the summation of the integrated loss densities in the different finite elements in the windings. However, a different approach is chosen for the massive (foil) windings and stranded windings.

- Foil windings: Both source and eddy current densities are present in the FEM magnetic field model. The total Joule loss is obtained by:

$$P_{foil} = R_{AC}(\omega)I^2 = \sum_e q_e = \sum_e \int_{\Omega_e} \frac{(J_s + j\omega\sigma A)^2}{\sigma} d\Omega \quad (13)$$

- Stranded windings: Since the eddy currents are neglected in this type of winding, only the *DC* losses are modelled. The contribution of the additional *AC* losses is to be estimated separately. This is accomplished by calculating the losses in an individual strand, subject to a leakage flux, modelled as a small massive conductor in additional FEM calculations. By varying the leakage flux strength, the additional loss function f_{ec} can be estimated and added [12]. This set of separate limited FEM calculations has to be performed only once for a certain strand dimension.

$$P_{wire} = R_{AC}(\omega)I^2 = \sum_e q_e = \sum_e \left(\frac{J_s^2}{\sigma} + f_{ec}(\omega).B^2 \right) \Omega_e \quad (14)$$

V. COUPLED PROBLEM COMPUTATION

The most flexible way to solve the global coupled problem consisting of the multiple magnetic field equations (6-7), the loss calculation routines (13-14), the thermal field equation (8) and the material characteristic corrections in every time step by means of the FEM, is block iteration (Fig. 3). This means that the subproblems are solved independently using specific efficient solvers with immediate re-use of the obtained intermediate results, until convergence. An alternative would be the construction of a Jacobian matrix in a Newton method. This yields a large ill-conditioned system to solve, in particular when several harmonics are involved. It is not always possible to derive the required partial derivatives.

Because of the diverse physical nature of the subproblems, not all the subproblems are solved on the same mesh. For instance, in the magnetic fields, air is meshed, whereas in the thermal field it is replaced by convective boundary conditions. To transfer the results from one mesh to another, projection or interpolation routines are used.

For steady-state problems, only the inner loop of the flow chart in Fig. 3 has to be solved. Transient problems require both loops. To overcome stiffness problems due to the difference in typical time constants of the magnetic and thermal problem, the 'transient frequency domain approach', as outlined above, has be used. As an approximation, the time derivative term could be skipped and a sort of quasi-steady-state problem is solved in every time step. However, this may lead to an unstable algorithm for large time steps as this implements a local extrapolation to a steady state, with the danger of overestimating loss values.

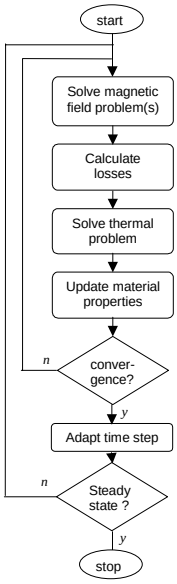

Fig. 3. Coupled problem computation flow chart.

VI. APPLICATION

A. Transient heating simulation

A 30 kVA transformer with 50 foil conductors as its secondary winding (closest to the core) is modelled in the described way. The primary winding is constructed of strands. The first order magnetic FEM model (Fig. 4) is constructed using adaptive refinement after domain based error estimation [13]. The real component of the magnetic field solution of the simulated short-circuit test is shown in Fig. 5. Fig. 6 shows a detail of the leakage field.

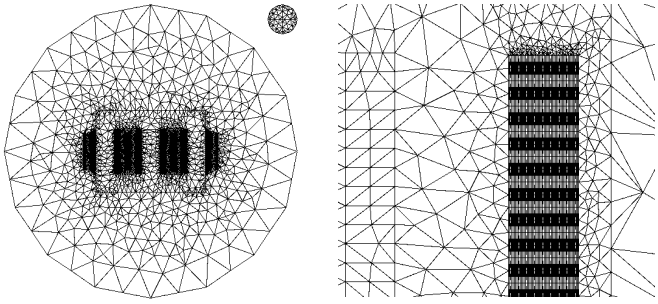

Fig. 4. FEM mesh and detail showing the fully meshed foil conductors.

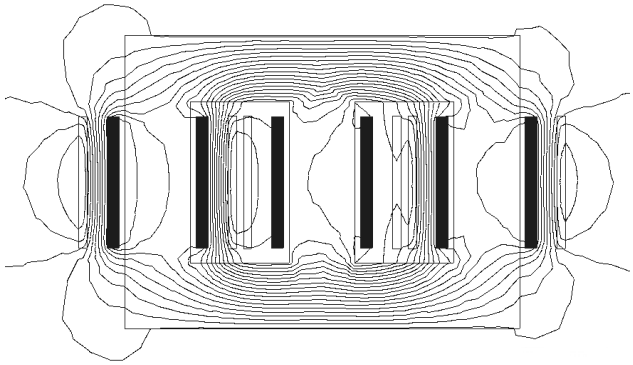

Fig. 5. Real part of the final magnetic field solution of a simulated short circuit test.

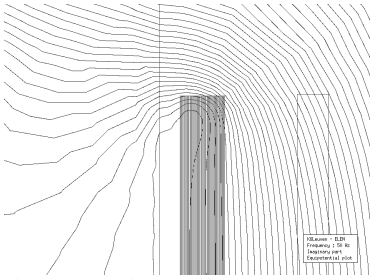

Fig. 6. Detail of the leakage flux; the field lines passing through the foil conductors in the top the coil are associated with additional eddy currents and losses at that location.

A short-circuit test simulation of the transformer operated by a sinusoidal voltage at 50 Hz is used to verify the approach. Due to the low core flux, saturation effects are negligible. inside the foils closest to the core high eddy currents are generated, shielding the outer foils. The surrounding air and the air between the windings is replaced by appropriate convection boundary conditions in the thermal model. Anisotropic materials are used for the foils. A detail of the solution is shown in Fig. 7, clearly indicating the location of the hot spot in the top of the foil winding coil.

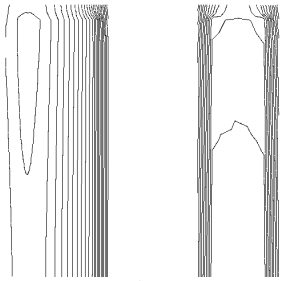

Fig. 7. Isothermal lines of the upper part of a coil set; on the left the foil conductor; on the right the wire coil.

To validate the transient simulations, measurements were performed and compared. Fig. 8 shows a good agreement. The difference between the steady-state temperature and the heating rate in the measurements and the simulation is explained by the difficult modelling of the natural convection cooling, especially for the coil parts within the yoke.

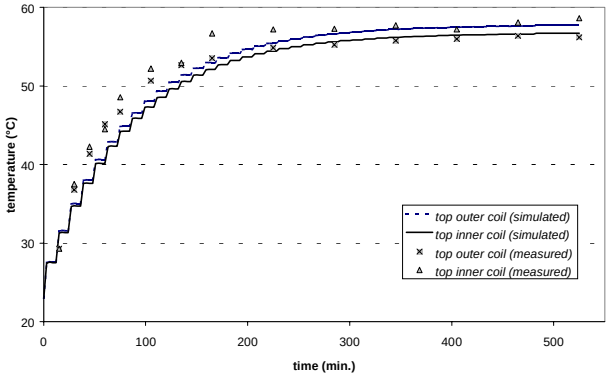

Fig. 8. Comparison of measured and calculated heating of the transformer in a short-circuit situation.

B. Thermal derating calculation

Simulations for different harmonic frequencies allow the determination of the additional losses due to power system harmonics. With this information, the increase of the hot spot temperature in the coils is simulated. This is illustrated by estimating the impact of a harmonic current spectrum (Fig. 9) on the transformer. The spectrum is obtained from measurements on high power electrical drive systems. It is limited to the 19th harmonic.

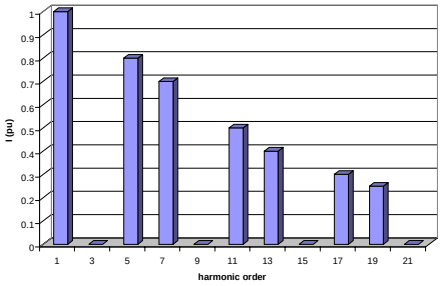

Fig. 9. Magnitude spectrum of the current harmonics.

In this 'hot spot derating test', in fact an optimisation problem, the steady-state temperature is calculated for several harmonic current magnitudes. The temperatures at the known locations of the hot spots is retrieved and plotted in Fig. 10 (the rightmost points indicate the non-derated current heating; the hot spots have a more than doubled temperature). The current magnitude for which the rated heating known from simulations with sinusoidal currents is reached, is interpolated. For load currents with the spectrum in Fig. 9, this is about 3.0 A; a thermally defined derating of almost 50 % is applicable.

The transient coupled algorithm can be used to study the heating effects under temporarily higher harmonics loads: in this way probable damage due to overload can be predicted.

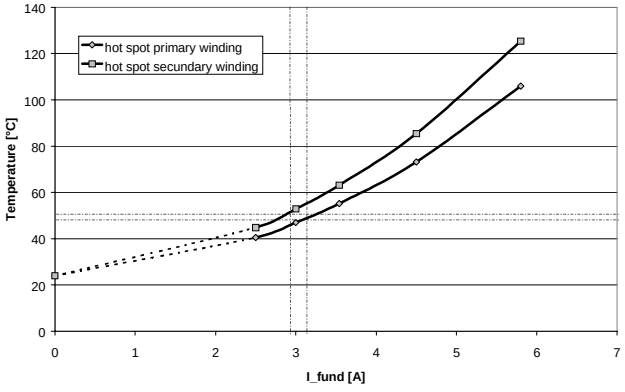

Fig. 10. Course of the hot spot temperatures as function of the fundamental current in the spectrum of Fig. 9; rated temperatures for a pure sinusoidal current are indicated.

VII. CONCLUSIONS

The coupled electromagnetic-thermal computation of transformers subject to power system harmonics is outlined. The calculation of the magnetic field in a mixed frequency and time domain approach is discussed, along with the thermal modelling and loss computation procedures. The solution of the constructed coupled problem is treated.

The methods are applied to a 30 kVA three-phase distribution transformer with a mixed stranded/foil winding. The transient heating up is compared with measurements. A thermal derating procedure, applicable in the design stage, using the computation model, is presented.

IX. REFERENCES

[1] I.Kerszenbaum, A.Mazur, M.Mistry and J.Frank, "Specifying dry-type distribution transformers for solid-state applications," IEEE Trans. Ind. Applicat., vol. 27, no.1, pp. 173-178, Jan./Feb. 1991.

[2] G.M.Massey, "Estimation Methods for power system harmonic effects on power distribution transformers," IEEE Trans. on Industry Applications, vol.30, no. 2, Mar./Apr. 1994, pp. 485-489.

[3] L.W.Pierce, "Transformer Design and Application Considerations for Nonsinusoidal Load Currents," IEEE Trans. on Ind. Appl., vol. 32, no. 3, May/June 1996, pp. 633-645.

[4] M.Bishop, J.Baranowki, D.Heath, S.Benna, "Evaluating harmonic-induced transformer heating," IEEE Trans. on Power Delivery, Jan. 1996, vol. 11, no.1, pp. 305-311.

[5] M.D.Hwang, W.M.Grady, H.W. Sanders Jr., "Calculation of Winding Temperatures in Distribution Transformers Subjected to Harmonic Currents," IEEE Trans. on Power Delivery, vol. 3, no. 3, July 1988.

[6] K. Hameyer, R. Belmans, *Numerical Modelling an Design of Electric Machines and Devices*, WIT-Press, 1999.

[7] J. Driesen, K. Hameyer, "Frequency Domain Finite Element Approximations for Saturable Electrical Machines under Harmonic Driving Conditions," to be published in COMPEL Journal, April 2000, 4p.

[8] E.M. Freeman, D.A. Lowther, "A Novel Mapping Technique for Open Boundary Finite Element Solutions to Poisson Equation," IEEE Trans. on Magnetics, vol. 24, no. 6, 1988, pp. 2934-2936.

[9] D. Lederer, A. Kost, "Modelling of Nonlinear Magnetic Material using a Complex Effective Refluctivity," IEEE Trans. on Magnetics , vol. 34, no. 5, 1998, pp. 3060-3063.

[10] J.H. Lienhard, *A Heat Transfer Textbook*, Prentice-Hall, Engelwood Cliffs, N.J., 1981.

[11] J.Driesen, R.Belmans, K.Hameyer, "Finite element modelling of thermal contact resistances and insulation layers in electrical machines," Proc. IEEE International Electric Machines and Drives Conference (IEMDC'99), Seattle, Washington, USA, 9-12.05.99, pp. 222-224.

[12] J. Driesen, K. Hameyer, "Practical Method to Determine Additional Load Losses due to Harmonic Currents in Transformers with Wire and Foil Windings," IEEE Power Engineering Society Winter Meeting, 23-27 January 2000, Singapore, 6 p.

[13] J. Driesen, G. Deliège, K. Hameyer, "Coupled thermo-magnetic simulation of a foil-winding transformer connected to a non-linear load," to be published in IEEE Trans. on Magnetics, September 2000, 4 pages.

VIII. BIOGRAPHIES

Johan Driesen (M'97) graduated in 1996 as Electrotechnical Engineer from the Katholieke Universiteit Leuven (KULeuven). Since 1996 he is a research assistant of the Fund for Scientific Research of Flanders (F.W.O.-Vl.). He received the 1996 R&D-award of the Belgian Royal Society of Electrotechnical Engineers (KBVE) for his Master Thesis on power quality problems. He is currently working towards the Ph.D. degree in Electrical Engineering at KULeuven. His research topics are the finite element solution of coupled thermal-electromagnetic problems and related applications in electrical machines and drives, microsystems and power quality issues.
J. Driesen is member of the Koninklijke Vlaamse Ingenieursvereniging (KVIV) and the IEEE.

Kay Hameyer (SM' 1995) received the M.S. degree in electrical engineering in 1986 from University of Hannover, Germany. He received the Ph.D. degree from University of Technology Berlin, Germany, 1992.
From 1986 to 1988 he worked with the Robert Bosch GmbH in Stuttgart, Germany, as a design engineer for permanent magnet servo motors. In 1988 he became a member of the staff at the University of Technology Berlin, Germany. From November to December 1992 he was a visiting professor at the COPPE Universidade Fderal do Rio de Janeiro, Brazil, teaching electrical machine design. In the frame of a collaboration with the TU Berlin, he was in June 1993 a visiting professor at the Université de Batna, Algeria. Beginning in 1993 he was a scientific consultant working on several industrial projects. From 1993 to March 1994, he held a HCM-CEAM fellowship financed by the European Community at the Katholieke Universiteit Leuven, Belgium. Currently he is professor for numerical field computations and electrical machines with the K.U.Leuven and a senior researcher with the F.W.O.-V. in Belgium, teaching CAE in electrical engineering and electrical machines. His research interests are numerical field computation, the design of electrical machines, in particular permanent magnet excited machines, induction machines and numerical optimization strategies.
Dr. Hameyer is member of the Koninklijke Vlaamse Ingenieursvereniging (KVIV), the International Compumag Society and the IEEE.

Ronnie J.M.Belmans (S'77-M'84-SM'89) received the M.S. degree in electrical engineering in 1979 and the Ph.D. in 1984, both from the Katholieke Universiteit Leuven, Belgium, the special Doctorate in 1989 and the Habilitierung in 1993, both from the RWTH Aachen, Germany.

Currently, he is a full professor with the K.U. Leuven, teaching electrical machines and CAD in magnetics. His research interests include electrical machine design (permanent magnet and induction machines), computer aided engineering and vibrations and audible noises in electrical machines. He was the director of the NATO Advanced Research Workshop on Vibrations and Audible Noise in Alternating Current Machines (August 1986). He was with the Laboratory for Electrical Machines of the RWTH Aachen, Germany, as a Von Humboldt Fellow (October 1988-September 1989). From October 1989 to September 1990, he was visiting professor at the McMaster University, Hamilton, ON., Canada. He obtained the chair of the Anglo-Belgian Society at the London University for the year 1995-1996.

Dr. Belmans is a member of the IEE (U.K.), the International Compumag Society and the Koninklijke Vlaamse Ingenieursvereniging (KVIV).